Available online at www.sciencedirect.com
SCIENCE DIRECT®
Journal of Sound and Vibration 288 (2005) 1177–1196
JOURNAL OF SOUND AND VIBRATION
www.elsevier.com/locate/jsvi

Concept and model of eddy current damper for vibration suppression of a beam

Henry A. Sodano[a,*], Jae-Sung Bae[b], Daniel J. Inman[a], W. Keith Belvin[c]

[a]*Center for Intelligent Materials Systems and Structures, Virginia Polytechnic Institute and State University, Blacksburg, VA 24061-0261, USA*
[b]*School of Aerospace and Mechanical Engineering, Hankuk Aviation University, 200-1, Hwajeon-dong, Deogyang-gu, Goyang-city, Geonggi-do, 412-791, Korea*
[c]*Structural Dynamics Branch, NASA Langley Research Center, Hampton, VA 23681-0001, USA*

Received 12 April 2004; received in revised form 12 January 2005; accepted 27 January 2005
Available online 29 March 2005

Abstract

Electromagnetic forces are generated by the movement of a conductor through a stationary magnetic field or a time varying magnetic field through a stationary conductor and can be used to suppress the vibrations of a flexible structure. In the present study, a new electromagnetic damping mechanism is introduced. This mechanism is different from previously developed electromagnetic braking systems and eddy current dampers because the system investigated in the subsequent manuscript uses the radial magnetic flux to generate the electromagnetic damping force rather than the flux perpendicular to the magnet's face as done in other studies. One important advantage of the proposed mechanism is that it is simple and easy to apply. Additionally, a single magnet can be used to damp the transverse vibrations that are present in many structures. Furthermore, it does not require any electronic devices or external power supplies, therefore functioning as a non-contacting passive damper. A theoretical model of the system is derived using electromagnetic theory enabling us to estimate the electromagnetic damping force induced on the structure. The proposed eddy current damper was constructed and experiments were performed to verify the precision of the theoretical model. It is found that the proposed eddy current damping mechanism could increase the damping ratio by up to 150 times and provide sufficient damping force to quickly suppress the beam's vibration.

*Corresponding author. Fax: +1 540231 2903.
E-mail address: hsodano@vt.edu (H.A. Sodano).

0022-460X/$ - see front matter © 2005 Elsevier Ltd. All rights reserved.
doi:10.1016/j.jsv.2005.01.016

Nomenclature

b	radius of the circular magnet
$\mathbf{B}$	magnetic flux density
B_r	residual magnetic flux
c_e	eddy current damping force
C	damping matrix
C_b	damping matrix of beam
δ	thickness of conductor
E	modulus of elasticity
$\mathbf{F}$	damping force
$\mathbf{J}$	eddy current density
$\mathbf{K}$	stiffness matrix
L	length of the magnet
l_g	gap length between magnet and conductor
$\mathbf{M}$	mass matrix
M_0	magnetization
μ_0	permeability of free space
ϕ	assumed mode shaped
ρ	density
Q_e	non-conservative forces
r	temporal coordinate
r_c	equivalent radius of the conductor
S	strain
σ	conductivity
t	time
$\mathbf{T}$	kinetic energy
u	displacement
$\mathbf{U}$	potential energy
v	velocity of conductor in z direction
$\mathbf{v}$	velocity of conductor
V	volume
ω_i	natural frequency

1. Introduction

When a non-magnetic conductive metal is placed in a magnetic field, eddy currents are generated. These eddy currents circulate in such a way that they induce their own magnetic field with opposite polarity of the applied field causing a resistive force. However, due to the electrical resistance of the metal, the induced currents will be dissipated into heat at the rate of I^2R and the force will disappear. In the case of a dynamic system the conductive metal is continuously moving in the magnetic field and experiences a continuous change in flux that induces an electromotive force (emf) allowing the induced currents to regenerate and in turn produce a repulsive force that is proportional to the velocity of the conductive metal. This process causes the eddy currents to function like a viscous damper and dissipate energy causing the vibrations to die out faster. The use of eddy currents for damping of dynamic systems has been known for decades and its application to magnetic braking systems [1–4] and lateral vibration control of rotating machinery [5,6] has been thoroughly investigated.

While the theory and applications of rotary magnetic braking systems have been well documented, there are many more applications of eddy current dampers. Karnopp [7] introduced the idea that a linear electrodynamic motor consisting of coils of copper wire and permanent magnets could be used as an electromechanical damper for vehicle suspension systems. It was shown that this actuator could be much smaller and lighter than conventional dampers while still providing effective damping in the frequency range typically encountered by road vehicle suspension systems; however it was unable to effectively isolate the vehicle from shock excitation. Schmid and Varga [8] studied a vibration-reducing system with eddy current dampers (ECDs) for high resolution and nanotechnology devices such as a scanning tunneling microscope (STM). Teshima et al. [9] investigated the effects of an eddy current damper on the vibrational characteristics of superconducting levitation and showed that the damping of vertical vibrations

was about 100 times improved by eddy current dampers. The concept of using a viscoelastic material to dissipate energy from a structure was modified to incorporated magnets by Oh et al. [10]. The study sandwiched a viscoelastic material between magnetic strips that were configured to attract each other in one case and to repel in the other. It was determined that the passive magnetic composite (PMC) treatments function best when the magnets were set to attract each other. However, this method of damping does not use eddy currents to apply damping to the structure.

Takagi et al. [11] studied the deflection of a thin copper plate subjected to magnetic fields both analytically and experimentally. They used an electromagnet with very high current (several hundred Amperes) to generate the magnetic field, then analyzed the response of the plate to the applied field. Kienholtz et al. [12] with CSA Engineering Inc. investigated the use of a magnetic tuned mass damper for vibration suppression of a spacecraft solar array and a magnetically damped isolation mount for the payload inside of a space shuttle. The magnetic tuned mass damper system targeted two modes of the solar array (1st torsion at 0.153 Hz and 1st out of plane bending of 0.222 Hz) and increased the damping by 30 and 28 dB, respectively, while the higher frequency untargeted modes 0.4–0.8 Hz were damped in the range of 11–16 dB. Matsuzaki et al. [13] proposed the concept of a new vibration control system in which the vibration of a beam, periodically magnetized along the span, is suppressed by using electromagnetic forces generated by a current passing between the magnetized sections. To confirm the vibration suppression capabilities of their proposed system, they performed a theoretical analysis of a thin beam with two magnetized segments subjected to an impulsive force and showed the concept to suppress the beams first three modes of vibration. Graves et al. [14] derived the mathematical model of electromagnetic dampers based on a motional emf and transformer emf devices and presented a theoretical comparison between these two devices. A motional emf device generates eddy currents due to the movement of a closed conduction circuit or a conductor through a stationary magnetic field, while a transformer emf device generates an emf within a stationary conducting circuit, due to a time-varying magnetic field. Both of these electromagnetic devices can be used for vibration damping purposes.

Recently, Kwak et al. [15] investigated the effects of an eddy current damper on the vibration of a cantilever beam and their experimental results showed that the eddy current damper can be an effective device for vibration suppression. The authors ECD uses a fixed copper conducting plate and flexible linkage attached to the tip of the beam in order to utilize the axial magnetic flux and generate eddy current damping forces. Bae et al. [16] modified and developed the theoretical model of the eddy current damper constructed by Kwak et al. [15]. Using this new model, the authors investigated the damping characteristics of the ECD and simulated the vibration suppression capabilities of a cantilever beam with an attached ECD numerically.

When using eddy currents the typical method of introducing an emf in the conductive metal is to place the metal directly between two oppositely poled magnets with the metal moving perpendicular to the magnets poling axis, a schematic of this process is shown in Fig. 1, and has been studied in Refs. [12,14–16]. This configuration is ideal because the magnetic field is concentrated between the two magnets causing the magnetic flux applied to the conductor to be greater and thus the damping force to be increased. While this configuration is effective for magnetic braking [1–4], in certain applications, such as the transverse vibration of a membrane, it is not possible. The research presented in this study analyzes one such system in which a vibrating cantilever beam is damped by a permanent magnet fixed to a location perpendicular to the beam's

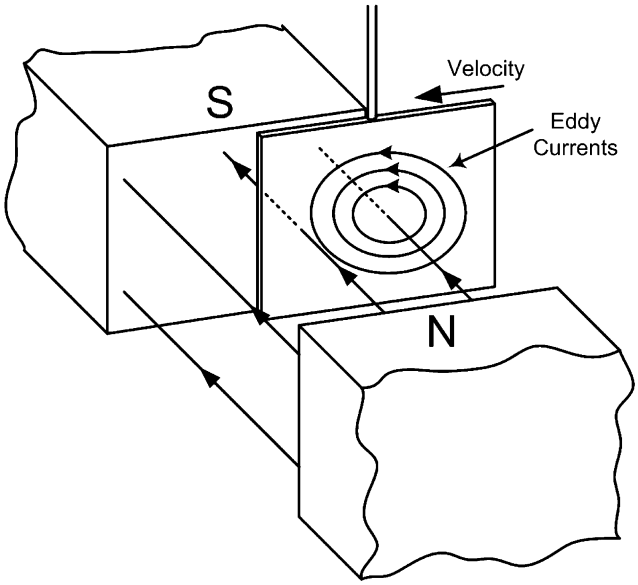

Fig. 1. Schematic of conductive material passing through a magnetic field and the generation of eddy currents.

motion and the magnet's radial flux is used to generate the damping force. Since the ECD of Ref. [15] was installed at the tip of the beam, its dynamic characteristics were changed considerably. Different from previous eddy current braking and damping systems, the proposed eddy current concept is to configure the ECD such that the beams motion is in line with the poling axis of the magnet. By arranging the magnet this way, the radial magnetic flux is used to generate the emf rather than the axial magnetic flux. Additionally, since the permanent magnet is not attached to the beam, the uncontrolled dynamic characteristics, other than the additional damping to the beam, are unaffected by the damper.

The following sections of this paper will use electromagnetic theory to identify the magnetic flux generated by a cylindrical permanent magnet. Following the determination of the magnetic flux, the eddy current distributions and the damping force due to the vibration of a cantilever beam will be found. Using the theoretical model of the proposed eddy current damping system, the vibration characteristics of a conductive beam subjected to a magnetic field are analytically determined. Following the development of the mathematical model of the system, experiments are performed to verify the accuracy of the eddy current damping model. It will be shown that the theoretical model provides an accurate prediction of the induced eddy current damping and the overall damping of the beam is shown to increased dramatically using this new system.

2. Eddy current damper and beam model

2.1. Eddy current damping force

Fig. 2 depicts the configuration of our eddy current damping system, which consist of a cantilever beam with a copper conducting plate located in the magnetic field generated by a single

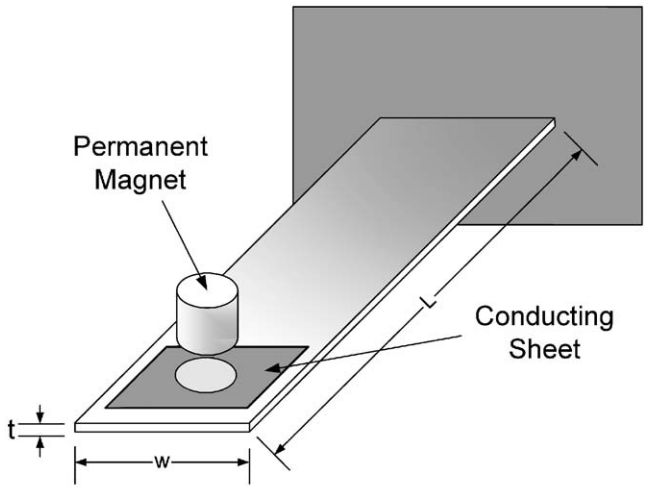

Fig. 2. Cantilever beam in magnetic field generated by permanent magnet.

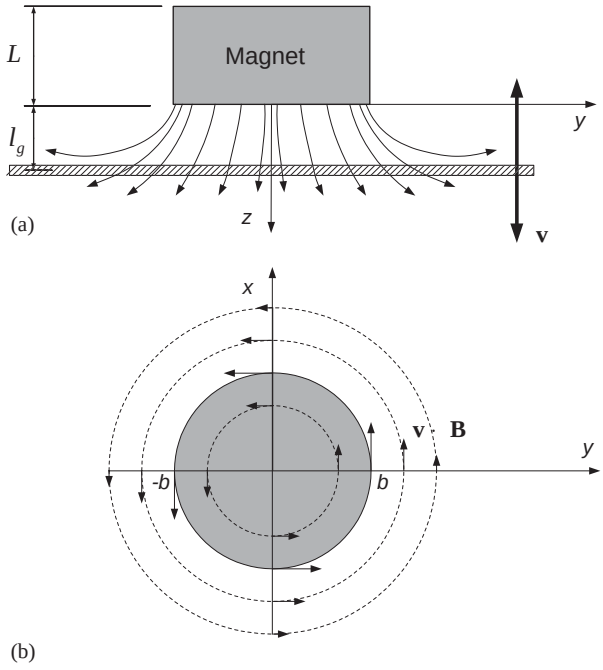

Fig. 3. (a) Magnetic field and (b) the eddy currents induced in the cantilever beam.

cylindrical permanent magnet. Due to the permanent magnet, a magnetic field is generated in the vertical (z) and horizontal or radial (y or R) axes. Fig. 3 shows a conducting sheet of thickness δ and conductivity σ moving with velocity $\mathbf{v}$ in the air gap l_g of a circular magnet. Due to the

permanent magnet, a magnetic field is generated in the vertical (z) and horizontal or radial (y or R) axes. When the beam surface is deflected and set in motion in the static magnetic field, an electric field is generated in the conducting sheet. Since the deflection of beam is in the vertical direction, the vertical component of the magnetic field does not contribute to the generation of eddy currents. Hence, the electric field on the conductor is dependent on the horizontal component B_y of the magnetic field. As shown in Fig. 3, the eddy currents circulate on the conducting sheet in the x–y plane, causing a magnetic field to be generated.

If the surface charges are assumed to be ignored, the current density $\mathbf{J}$ induced in the conducting sheet moving in the vertical direction is given by

$$\mathbf{J} = \sigma(\mathbf{v} \times \mathbf{B}), \tag{1}$$

where the $\mathbf{v} \times \mathbf{B}$ term is an electromotive force driving the eddy currents $\mathbf{J}$.

The magnetic flux density due to a circular magnetized strip, shown in Fig. 4, can be written as [17]

$$\mathrm{d}\mathbf{B} = \frac{\mu_0 M_0}{4\pi} \int_0^{2\pi} \frac{\mathrm{d}\mathbf{l} \times \mathbf{R}_1}{R_1^3} \, \mathrm{d}\phi, \tag{2}$$

where μ_0 and M_0 are the permeability and the magnetization per unit length, respectively. The vector $\mathbf{R}_1$ is defined by the distance between the differential element on the circular strip and the point on the y–z plane as shown in Fig. 4 and defined as

$$\mathbf{R}_1 = \mathbf{R} - \mathbf{r}, \tag{3}$$

where

$$\mathbf{R} = y\mathbf{j} + z\mathbf{k}, \quad \mathbf{r} = b\cos\phi\mathbf{i} + b\sin\phi\mathbf{j}. \tag{4,5}$$

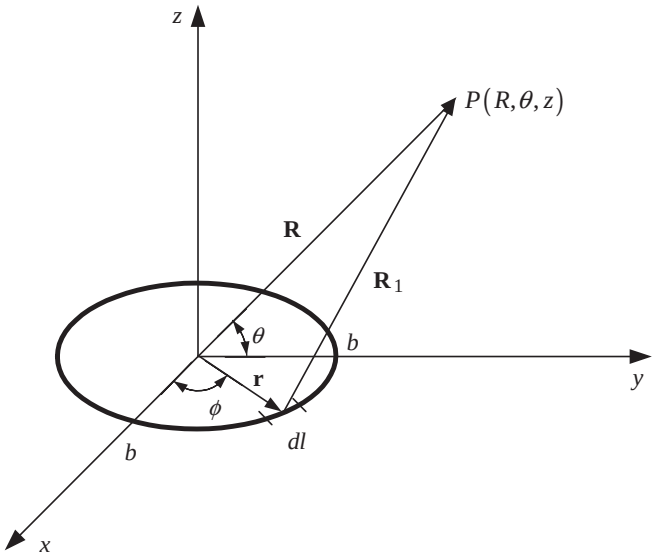

Fig. 4. Schematic of the circular magnetized strip depicting the variable used in the analysis.

The length vector $d\mathbf{l}$ of the infinitesimal strip is

$$d\mathbf{l} = -b\sin\phi\, d\phi\mathbf{i} + b\cos\phi\, d\phi\mathbf{j}, \tag{6}$$

where b is the radius of the circular magnet.

Substituting Eqs. (3) and (6) into Eq. (2), the magnetic flux density due to the circular magnetized strip is

$$B_y = \frac{\mu_0 z M_0 b}{4\pi}\int_0^{2\pi}\frac{\sin\phi}{(b^2+y^2+z^2-2yb\sin\phi)^{3/2}}\,d\phi = \frac{\mu_0 z M_0 b}{4\pi}\,I_1(b,y,z), \tag{7}$$

$$B_z = \frac{\mu_0 M_0 b}{4\pi}\int_0^{2\pi}\frac{b-y\sin\phi}{(b^2+y^2+z^2-2yb\sin\phi)^{3/2}}\,d\phi = \frac{\mu_0 M_0 b}{4\pi}\,I_2(b,y,z), \tag{8}$$

where I_1 and I_2 include the elliptic integrals and are shown in Appendix A. Hence, the magnetic flux densities due to the circular magnet of length L are written as

$$B_y(y,z) = \frac{\mu_0 M_0 b}{4\pi}\int_{-L}^{0}(z-z')I_1(b,y,z-z')\,dz', \tag{9}$$

$$B_z(y,z) = \frac{\mu_0 M_0 b}{4\pi}\int_{-L}^{0} I_2(b,y,z-z')\,dz', \tag{10}$$

where z' and L are the distance in the z direction from the center of a magnetized infinitesimal strip and the length of the circular magnet, respectively. As shown in Fig. 2, the magnetic field distributions in Eqs. (9) and (10) are symmetric about the z-axis.

Since the velocity of the conducting sheet is in the z direction, the magnetic flux density B_z does not contribute to the damping force. Using Eqs. (1), (9), and (10), the damping force due to the eddy current is defined by

$$\mathbf{F} = \int_V \mathbf{J}\times\mathbf{B}\,dV = -\mathbf{k}\sigma\delta v\int_0^{2\pi}\int_0^{r_c} yB_y^2(y,l_g)\,dy\,d\phi = -\mathbf{k}2\pi\sigma\delta v\int_0^{r_c} yB_y^2(y,l_g)\,dy, \tag{11}$$

where δ and v are the thickness and the vertical velocity of the conducting sheet, respectively, r_c is the equivalent radius of the conductor that preserves its surface area and l_g is the distance between the conducting sheet and the bottom on the magnet as shown in Fig. 3. Since the magnetic flux densities in Eqs. (9) and (10) are symmetric about the z-axis, the x and y component of the damping force are zero. Because Eqs. (7)–(11) cannot be analytically integrated, a numerical integration method will be used to obtain the damping force in Eq. (11).

2.2. Modeling of cantilever beam

In order to model the dynamics of the cantilever beam, energy methods were used. To begin the derivation the kinetic energy, potential energy and external work are written as

$$T = \frac{1}{2}\int_V \rho\dot{u}(x,t)^{\mathrm{T}}\dot{u}(x,t)\,dV, \quad U = \frac{1}{2}\int_V \underline{S}^{\mathrm{T}}E\,\underline{S}\,dV, \tag{12,13}$$

$$F\delta x = Q_e\delta u(x_e) + \sum_{i=1}^{nf} \delta \underline{u}(x_i) \cdot \underline{f_i}(x_i), \tag{14}$$

where $u(x,t)$ is the displacement of the beam, ρ is the density, V is the volume of the beam, f_i is the ith concentrated force acting on the beam, E is the modulus of elasticity and S is the strain of the beam. The term Q_e describes the non-conservative forces due to the induced eddy currents and is written as

$$Q_e\delta u(x_e) = -\int_0^L \delta u(x,t)^{\mathrm{T}} c_b \dot{u}(x,t)\,\mathrm{d}x - c_e\delta u(x_e,t), \tag{15}$$

where c_b is the internal damping of the beam, L is the length of the beam and c_e and u_e are the damping force from the eddy currents and the location of the eddy current damping force, respectively. By Hamilton's Principle the variation of the energy in the system must balance to zero as follows:

$$\int_{t_1}^{t_2} [\delta U + \delta T - F\delta x]\,\mathrm{d}t = 0. \tag{16}$$

Taking the variation of the kinetic and potential energy from Eq. (16) yields

$$\delta U = \int_V \delta \underline{S}^{\mathrm{T}} E\,\underline{S}\,\mathrm{d}V, \quad \delta T = \int_V \rho\delta\dot{u}^{\mathrm{T}}\dot{u}\,\mathrm{d}V. \tag{17,18}$$

The variations found in Eqs. (14), (17) and (18) can be substituted into Eq. (16) to obtain the variational equation

$$\int_{t_1}^{t_2}\left[\int_V \rho\delta\dot{u}^{\mathrm{T}}\dot{u}\,\mathrm{d}V - \int_V \delta\underline{S}^{\mathrm{T}} E\,\underline{S}\,\mathrm{d}V + \sum_{i=1}^{nf} \delta\underline{u}(x_i)\cdot\underline{f_i}(x_i) - \int_0^L \delta\dot{u}^{\mathrm{T}} c_b\dot{u}\,\mathrm{d}x - c_e\delta\dot{u}(x_e,t)\right] = 0. \tag{19}$$

In order to solve Eq. (19) for the cantilever beam some assumptions must be made. The first assumption follows the Rayleigh–Ritz procedure (see for instance Ref. [18]), which says that the displacement of the beam can be written as the summation of modes in the beam and a temporal coordinate

$$u(x,t) = \sum_{i=1}^{N} \phi_i(x) r_i(t) = \underline{\phi}(x)\,\underline{r}(t), \tag{20}$$

where $\phi_i(x)$ are the assumed mode shapes of the structure which can be set to satisfy any combination of boundary conditions, $r(t)$ is the temporal coordinate of the displacement and N is the number of modes to be included in the analysis. The second assumption made is to apply the Euler–Bernoulli beam theory. This allows the strain in the beam to be written as the product of the distance from the neutral axis and the second derivative of displacement with respect to the position along the beam. Once the strain is defined in this way Eq. (20) can be used to define the

strain as

$$\underline{S} = -y\,\frac{\partial^2 u(u,t)}{\partial x^2} = -y\,\underline{\phi}(x)''\,\underline{r}(t), \tag{21}$$

where y is the distance from the neutral axis of the beam. Using the previous two assumptions, Eq. (19) can be simplified to contain terms that represent physical parameters. By doing this, the equations representing the beam become more recognizable when compared to those of a typical system and help give physical meaning to the parameters in the equation of motion. The mass and stiffness matrix of the system can be written as

$$M = \int_V \rho \underline{\phi}^{\mathrm{T}}(x)\,\underline{\phi}(x)\,\mathrm{d}V, \quad \int_V y^2 \underline{\phi}^{\mathrm{T}}(x)''E\,\underline{\phi}(x)''\,\mathrm{d}V. \tag{22,23}$$

The non-conservative forces that include the internal damping of the beam and the eddy current damping force can be written as the damping matrix defined by

$$C = \int_V \underline{\phi}^{\mathrm{T}}(x) c_b\,\underline{\phi}(x)\,\mathrm{d}V + \mathrm{diag}[c_e\,\underline{\phi}(x_e)], \tag{24}$$

where $\phi(x_e)$ is the modes shape with x_e defining the location of the eddy current damping force and c_e is the damping force found in Eq. (11). The parameters defined in Eqs. (22)–(24) can be substituted into Eq. (19). This substitution allows the variation to be written as

$$\int_1^{t_2} [\delta\underline{\dot{r}}^{\mathrm{T}}(t)\mathbf{M}\,\underline{\dot{r}}(t) - \delta\underline{r}^{\mathrm{T}}(t)\mathbf{K}\,\underline{r}(t) - \delta\underline{\dot{r}}^{\mathrm{T}}(t)\mathbf{C}\,\underline{\dot{r}}(t) + \delta\,\underline{r}(t)\phi(x_i)^{\mathrm{T}}\underline{f}(t)]\,\mathrm{d}t = 0, \tag{25}$$

where $\delta()$ indicates the variation of the corresponding variable. Taking the integral of Eq. (25) leaves the equation of motion. The following equation defines the motion of the beam with the eddy current damper:

$$M\,\underline{\ddot{r}}(t) + C\,\underline{\dot{r}}(t) + K\,\underline{r}(t) = \underline{\phi}(x_i)^{\mathrm{T}}\underline{f}_i(t). \tag{26}$$

The above equations now describe the dynamics of the beam and its interaction with the eddy current damper. One point that must be mentioned is that the eddy current damping force is highly nonlinear with respect to the gap between the magnet and the beam. However, in the derivation of the beam's dynamics with the eddy current damper, the damping force was assumed to be a constant value corresponding to the mean distance between the magnet and beam. In the following sections both the accuracy of the modeling techniques used and this assumption will be demonstrated.

3. Experimental set-up

In order to validate the accuracy of the model, experiments were performed on an aluminum beam with dimensions shown in Fig. 5. For all tests performed a neodymium–iron–boron permanent magnet with radius and length of 6.35 and 12.7 mm, respectively, was used. The other

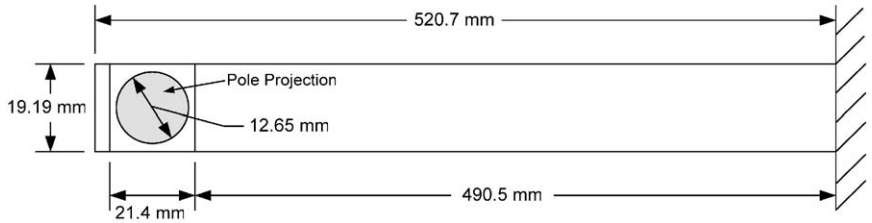

Fig. 5. Schematic showing the dimensions of the beam.

Table 1
Physical properties of the beam, conductor and magnet

Property	Value
Young's modulus of beam	75 GPa
Density of beam	2700 kg/m^3
Conductivity of beam	3.82×10^7
Thickness of copper conductor	0.62 mm
Conductivity of copper conductor	5.80×10^7
Permanent magnet composition	NdFeB 35
Residual magnetic flux of magnet	1.21 kG

physical properties of the beam, conductor and magnet are listed in Table 1. When performing the validation of the model, it was necessary to include the eddy currents generated from the aluminum beam in the simulation as well, because of its high conductivity.

The goal of these experiments was to measure the damping of the beam as a function of the gap l_g between the copper conducting plate and the surface of the permanent magnet. To do this both the response to an initial displacement and the frequency response were measured. From these two tests the damping of the beam can be calculated by determining the logarithmic decrement of the initial condition response and the unified matrix polynomial approach (UMPA) can be applied to the frequency response. It was necessary to find the damping using both of these methods because the eddy currents add significant damping when the magnet is placed in close proximity to the beam, making the damping measurement difficult.

In order to accurately measure the damping of the aluminum beam using an initial displacement and the log decrement method, the initial condition must be consistent throughout all tests. This is necessitated further due to the need to measure the damping for numerous different gap distances l_g for the magnet and conducting plate. Therefore to ensure that the initial displacement was consistent throughout every test a very thin steel plate was attached to the beam and an electromagnet was positioned at a fixed distance from the beam and steel plate. A small switch was constructed to allow the magnet to be activated and thus pull the steel plate into contact with the surface of the electromagnet and provide a fixed initial displacement. When the switch was turned off the electromagnet releases the beam allowing its vibration to damp out, this system can be seen in Fig. 6. Once the beam is set into motion, a Polytec laser vibrometer was used to measure the displacement of the tip of the beam.

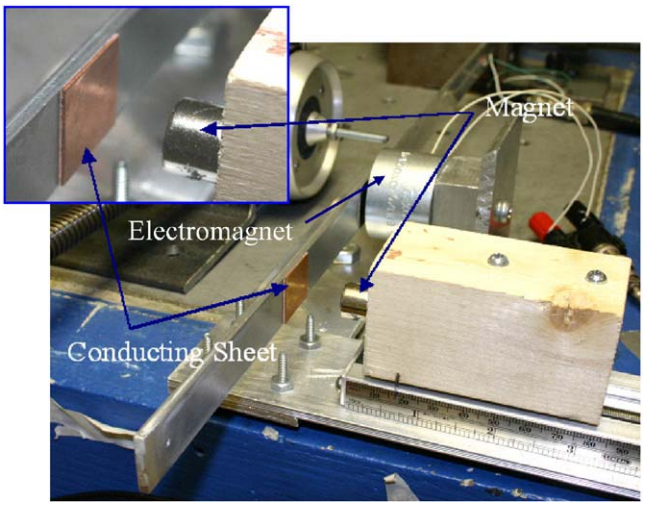

Fig. 6. Experimental set-up of the aluminum beam and eddy current damper.

To measure the frequency response of the aluminum beam, a piezoelectric patch was attached to the root of the beam while the beam's response was measured using a Polytec laser vibrometer. With the two excitation systems developed, the next step was to construct an accurate method of positioning the permanent magnet a fixed distance from the conducting plate. To do this, the permanent magnet was bonded to a wooden block that was fixed to a fine threaded lead screw, as shown in Fig. 6, this lead screw allowed the position of the magnet to be accurately varied. A wooden block was used so that the magnetic field was not distorted due to high permeability materials in close proximity to the magnet. The combination of a lead screw for positioning, fixed electromagnet for consistent initial displacement, permanently bonded piezoelectric patch and a non-contact sensing system (laser vibrometer) allowed every test to be precisely repeated.

4. Comparison of model and experiments

4.1. Numerical calculation of the magnetic flux

Following the construction of the experimental set-up the accuracy of the model could be shown. However, before the damping force generated by the eddy currents and the beam response could be found the magnetic field of the permanent magnet had to be calculated. Because Eqs. (9) and (10) cannot be solved analytically they were numerically integrated. The resulting magnetic flux **B** of this integration is shown in Fig. 7, for the case of a cylindrical permanent magnet with length L and whose surface is located at $z = 0$. The contours in Fig. 7 indicate the radial component B_y of the magnetic flux. Since the conductor moves in the z direction, the z component B_z of the magnetic flux does not contribute to the generation of eddy currents in the conductive material, indicating that only the radial component B_y affects the strength of the eddy current flowing through the conducting sheet. Fig. 8 shows the radial magnetic flux density distribution when the conducting sheet is at various distances from the magnetic surface. It is apparent that as

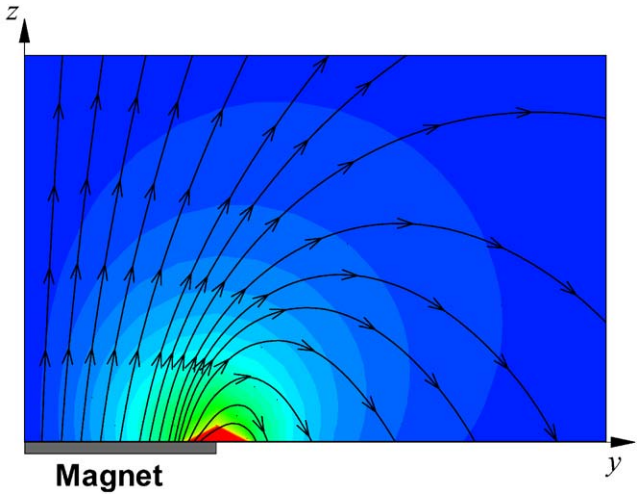

Fig. 7. Magnetic flux and contour of B_y for case of single pole.

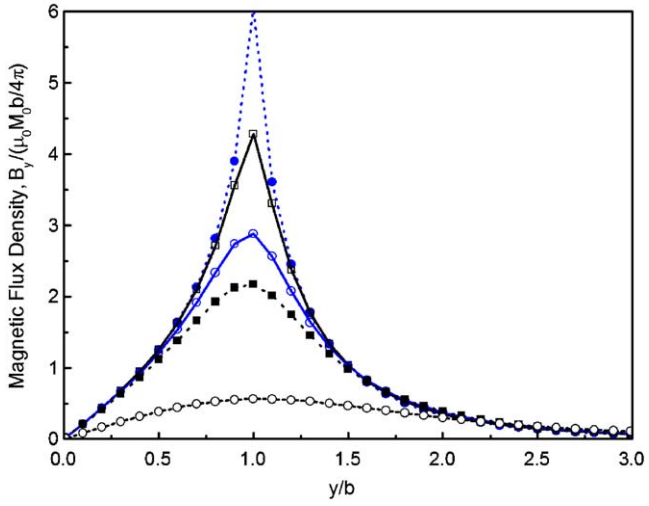

Fig. 8. Magnetic density distributions in y direction. Key: - -●- -, $l_g/b = 0.05$; –□–, $l_g/b = 0.1$; –○–, $l_g/b = 0.2$; - -■- -, $l_g/b = 0.3$; - -○- -, $l_g/b = 1.0$.

the distance l_g between the magnet and the conducting sheet decreases, the magnetic flux density increases. Additionally, Fig. 8 shows that the maximum value of the radial magnetic flux density B_y occurs at the boundary of the circular magnet.

4.2. Validation of model of eddy current damping

Following the determination of the magnetic flux, the dynamics of the beam and eddy current damper could be combined and compared to those obtained through experiments. Using the

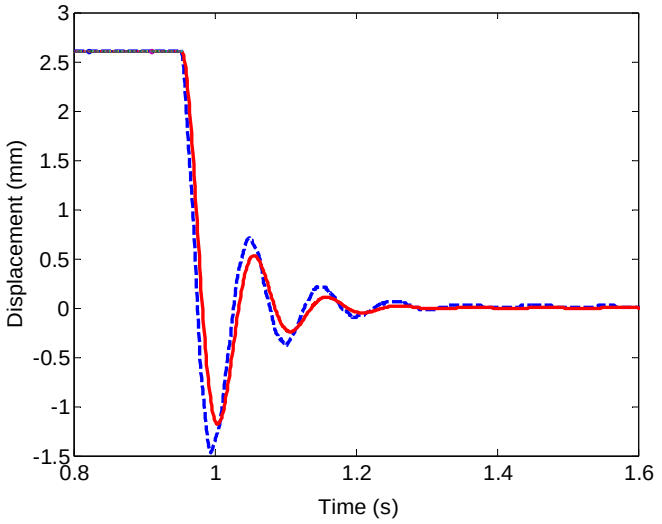

Fig. 9. Experimental and predicted beam response to an initial displacement with magnet located at a distance of 2 mm. Key: - -, measured; -, predicted.

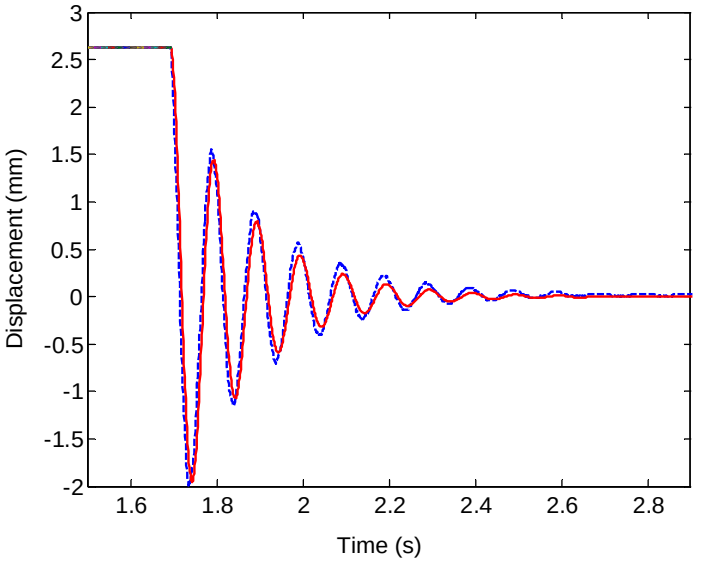

Fig. 10. Experimental and predicted beam response to an initial displacement with magnet located at a distance of 4 mm. Key: - -, measured; -, predicted.

initial displacement experiments, the log decrement was calculated to provide the damping of the aluminum beam when subjected to the magnetic field of a permanent magnetic positioned at numerous distances l_g from the conducting plate. Fig. 9 shows the beam response to an initial

condition for the case that the surface of the permanent magnet is located at a distance of 2 mm from the conducting plate and Fig. 10 shows the response of the beam when the magnet is located at a distance of 4 mm. From these figures it is apparent that the damping of the beam is significantly increased due to the interaction between the eddy currents and the magnet, in the case that the magnet was not present, the settling time of the beam would be on the order to 1 min rather than a fraction of a second. Additionally, these figures demonstrate the accuracy of the model. When the initial displacement tests were performed, the smallest distance from the beam that the magnet could be placed at was 1.0 mm in order to avoid the beam coming in contact with the magnet during its response. By adjusting the gap between the magnet and beam the damping ratio as a function of the distance was measured.

Furthermore, to demonstrate the effectiveness of this non-contacting magnetic damper for the suppression of the transverse vibrations of a beam, experiments were performed to determine the frequency response before and after placement of the magnet; the results of this test are shown in Fig. 11. Fig. 11 shows that the first mode of vibration is significantly reduced by approximately 42.4 dB and the second and third mode are suppressed by 21.9 and 14.3 dB, respectively. The frequency response of the beam was determined for various gaps between the magnet and beam ranging from 1 to 10 mm so that the model's accuracy could be demonstrated. Fig. 12 shows the experimental and predicted frequency response of the beam with the magnet located 2 mm from the beam. Fig. 12 shows that the dynamics of the beam are well characterized by the model. Using the experimental results, the damping of the beam as the distance between the magnet and beam was increased was calculated using the UMPA method. With the measured damping ratio from both the initial displacement and frequency response experiments we were able to use the damping force calculated in Eq. (11) to determine the predicted values of damping; the results of the

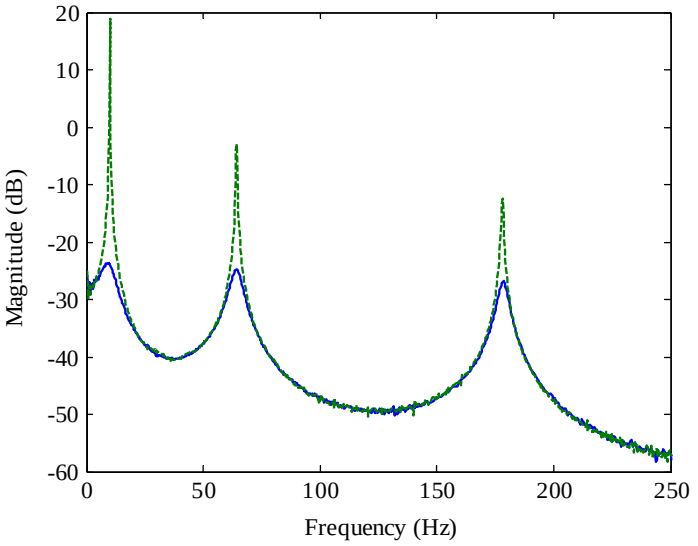

Fig. 11. Experimentally measured damped and undamped frequency response of the beam. Key: - -, undamped; -, damped.

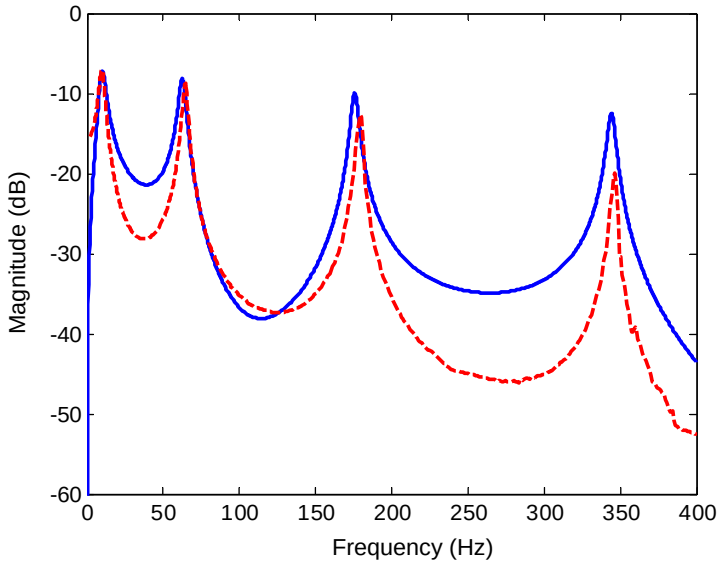

Fig. 12. Predicted and experimentally measured frequency response of the beam with the magnet at a distance of 2 mm. Key: -, experimental; - -, predicted.

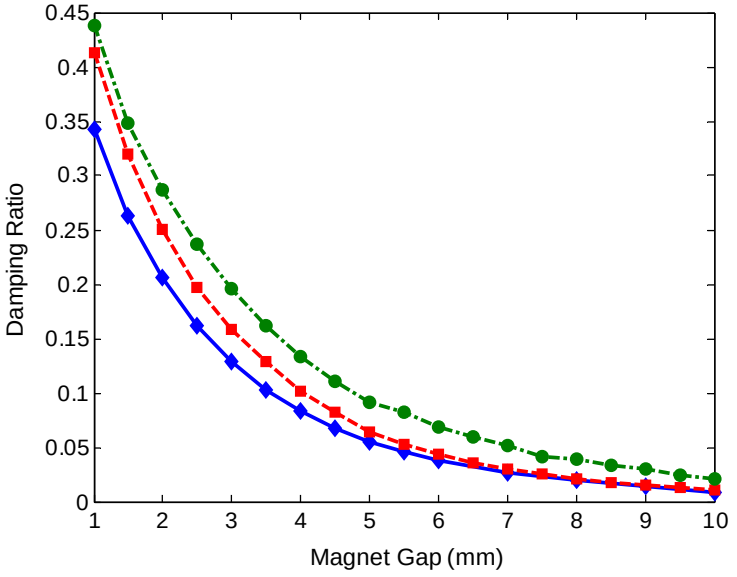

Fig. 13. Experimental and predicted damping ratio of the first mode as a function of the gap between the magnet and beam. Key: -●-, infinite conductor; -■-, finite conductor; -◇-, experimental.

experiments and model for the first mode of vibration are shown in Fig. 13. Fig. 13 shows two curves for the estimated damping ratio. The infinite conductor curve represents the damping that would be expected if the conducting plate was of infinite dimensions and corresponds to setting r_c

in Eq. (11) equal to infinity, and the second curve defines the damping ratio resulting in the case where the conductor is of the finite size used in the experiments. It can be seen that the model provides an accurate estimate of the damping ratio and as the distance increases, the model converges to the measured damping of the beam. The average predicted damping over the entire range of gaps tested is approximately 17%, however the accuracy of the model in the range greater than 5 mm is less than 10%. The experimental and predicted damping ratios for the second through the fourth mode are shown in Appendix B.

While this model does provide an accurate estimate of the damping due to the eddy currents generated in the beam there are a few sources of error that can be improved. First the conductor applied to the beam is not of circular geometry as assumed in the analysis and second the edge effects of the conducting plate are not represented due to the eddy current density at the conductor's edge not being zero. If the geometry of the conducting plate in our analysis was modified to be rectangular, it is expected that the model would provide a more accurate prediction of the damping for the case that the magnet is only a small distance from the magnet. Additional sources of error arise due to the relatively small size of the conducting plate compared to the surface of the magnet.

5. Conclusions

This study has introduced the concept of an eddy current damper to suppress the transverse vibrations of a cantilever beam. Unlike constrained layer damping or other damping techniques which significantly affect the structures response after their application; this damping scheme is easy to install and functions in a non-contact fashion thus allowing mass loading and added stiffness that are common to most damping techniques to be avoided by its addition to the system. This point is a crucial one for systems that have been designed with a specific dynamic response, yet require additional damping subsequent to their design. Other methods of damping would alter the desired performance (e.g. the systems natural frequencies and mode shapes) of the system, while the eddy current damper developed in the present study would not.

A theoretical model of the system was derived using electromagnetic theory, enabling the electromagnetic damping force induced on the structure to be estimated. The proposed eddy current damper was constructed and experiments were performed to verify the precision of the theoretical model. The model was shown to provide an accurate estimate of the induced damping. It has been found that the proposed eddy current damping mechanism could increase the damping ratio by up to 150 times and provide sufficient damping force to quickly suppress the beam's vibration.

Acknowledgements

The first author of this paper gratefully acknowledges support from NASA's Graduate Student Researchers Program (GSRP) under Grant number NGT-1-03020 with the direction of W.K. Belvin from NASA Langley Research Center.

Appendix A. Integrals defining the magnetic flux

The integration I_1 in Eq. (7) is

$$I_1 = \int_0^{2\pi} \frac{\sin\phi}{(b^2+z^2-2yb\sin\phi)^{2/3}}\,\mathrm{d}\phi = \frac{1}{bynp^2}\left[m^2\left\{E_1\left(\frac{\pi}{4},\frac{-4yb}{n^2}\right)+E_1\left(\frac{3\pi}{4},\frac{-4yb}{n^2}\right)\right\}-p^2\left\{E_2\left(\frac{\pi}{4},\frac{-4yb}{n^2}\right)+E_2\left(\frac{3\pi}{4},\frac{-4yb}{n^2}\right)\right\}\right], \tag{A.1}$$

where

$$m^2 = b^2+y^2+z^2, \quad n^2 = (b-y)^2+z^2, \quad p = (b+y)^2+z^2. \tag{A.2–A.4}$$

The elliptic integrals of Eq. (A.1) are

$$E_1 = (\phi,m) = \int_0^{\phi}(1-m\sin^2\theta)^{1/2}\,\mathrm{d}\theta, \tag{A.5}$$

$$E_2 = (\phi,m) = \int_0^{\phi}(1-m\sin^2\theta)^{-1/2}\,\mathrm{d}\theta. \tag{A.6}$$

The integration I_2 in Eq. (8) is

$$I_2 = \int_0^{2\pi} \frac{b-y\sin\phi}{(b^2+z^2-2yb\sin\phi)^{2/3}}\,\mathrm{d}\phi = \frac{1}{bnp^2}\left[s\left\{E_1\left(\frac{\pi}{4},\frac{-4yb}{n^2}\right)+E_1\left(\frac{3\pi}{4},\frac{-4yb}{n^2}\right)\right\}+p^2\left\{E_2\left(\frac{\pi}{4},\frac{-4yb}{n^2}\right)+E_2\left(\frac{3\pi}{4},\frac{-4yb}{n^2}\right)\right\}\right], \tag{A.7}$$

where

$$m^2 = b^2+y^2+z^2, \quad n^2 = (b-y)^2+z^2, \tag{A.8,A.9}$$

$$p = (b+y)^2+z^2, \quad s = b^2-y^2-z^2. \tag{A.10,A.11}$$

The elliptic integrals of Eq. (A.7) are

$$E_1 = (\phi,m) = \int_0^{\phi}(1-m\sin^2\theta)^{1/2}\,\mathrm{d}\theta, \tag{A.12}$$

$$E_2 = (\phi,m) = \int_0^{\phi}(1-m\sin^2\theta)^{-1/2}\,\mathrm{d}\theta. \tag{A.13}$$

Appendix B

Predicted and measured damping ratios of higher modes are shown in Figs. B.1–B.3.

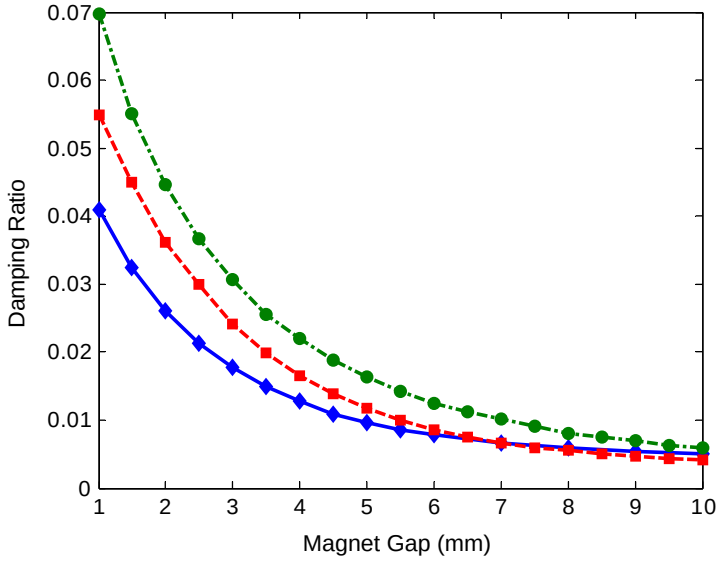

Fig. B.1. Experimental and predicted damping ratio of the second mode as a function of the gap between the magnet and beam. Key: -●-, infinite conductor; -■-, finite conductor; -◇-, experimental.

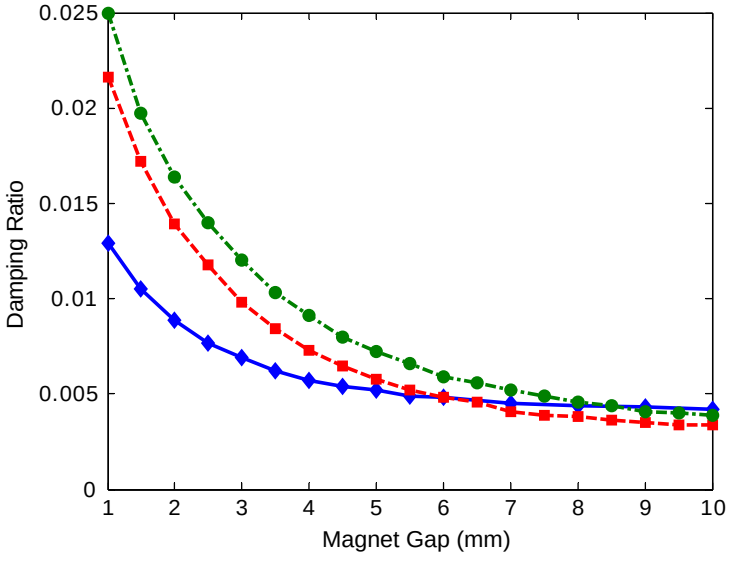

Fig. B.2. Experimental and predicted damping ratio of the third mode as a function of the gap between the magnet and beam. Key: -●-, infinite conductor; -■-, finite conductor; -◇-, experimental.

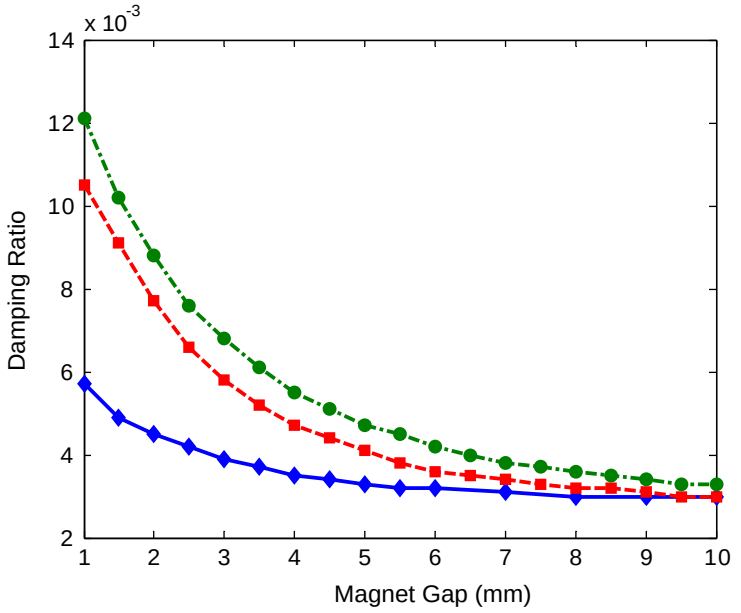

Fig. B.3. Experimental and predicted damping ratio of the fourth mode as a function of the gap between the magnet and beam. Key: -●-, infinite conductor; -■-, finite conductor; -◇-, experimental.

References

[1] H.H. Wiederick, N. Gauthier, D.A. Campbell, Magnetic braking: simple theory and experiment, *American Journal of Physics* 55 (1987) 500–503.
[2] M.A. Heald, Magnetic braking: improved theory, *American Journal of Physics* 56 (1988) 521–522.
[3] L.H. Cadwell, Magnetic damping: analysis of an eddy current brake using an airtrack, *American Journal of Physics* 64 (1996) 917–923.
[4] K.J. Lee, K.J. Park, A contactless eddy current brake system, *IEEE Conference on Intelligent Processing Systems*, Australia, December 1998, pp. 193–197.
[5] G. Genta, C. Delprete, A. Tonoli, E. Rava, L. Mazzocchetti, Analytical and experimental investigation of a magnetic radial passive damper, in: *Proceedings of the Third International Symposium on Magnetic Bearings*, 1992, pp. 255–264.
[6] Y. Kligerman, A. Grushkevich, M.S. Darlow, A. Zuckerberger, Analysis and experimental evaluation of inherent instability in electromagnetic eddy-current dampers intended for reducing lateral vibration of rotating machinery, in: *Proceedings of ASME, 15th Biennial Conference on Vibration and Noise*, Boston, MA, 1995, pp. 1301–1309.
[7] D. Karnopp, Permanent magnet linear motors used as variable mechanical damper for vehicle suspensions, *Vehicle System Dynamics* 18 (1989) 187–200.
[8] M. Schmid, P. Varga, Analysis of vibration-isolating systems for scanning tunneling microscopes, *Ultramicroscopy* 42–44 (1992) 1610–1615.
[9] H. Teshima, M. Tanaka, K. Miyamoto, K. Nohguchi, K. Hinata, Effect of eddy current dampers on the vibrational properties in superconducting levitation using melt-processed YbaCuO bulk superconductors, *Physic C* 274 (1997) 17–23.
[10] L. Oh, M. Ruzzene, A. Baz, Control of the dynamic characteristics of passive magnetic composites, *Composites Part B: Engineering* 30 (1999) 739–751.

[11] T. Takagi, J. Tani, S. Matsuda, S. Kawamura, Analysis and experiment of dynamic deflection of a thin plate with a coupling effect, *IEEE Transactions on Magnetics* 28 (1992) 1259–1262.
[12] D.A. Kienholtz, S.C. Pendleton, K.E. Richards, D.R. Morgenthaler, Demonstration of solar array vibration suppression, *Proceedings of SPIE's Conference on Smart Structures and Materials*, vol. 2193, Orlando, FL, February 14–16, 1994, pp. 59–72.
[13] Y. Matsuzaki, Y. Ishikubo, T. Kamita, T. Ikeda, Vibration control system using electromagnetic forces, *Journal of Intelligent Material Systems and Structures* 8 (1997) 751–756.
[14] K.E. Graves, D. Toncich, P.G. Iovenitti, Theoretical comparison of motional and transformer EMF device damping efficiency, *Journal of Sound Vibration* 233 (2000) 441–453.
[15] M.K. Kwak, M.I. Lee, S. Heo, Vibration suppression using eddy current damper, *Korean Society for Noise and Vibration Engineering* 13 (10) (2003) 760–766.
[16] J.S. Bae, M.K. Kwak, D.J. Inman, Vibration suppression of cantilever beam using eddy current damper, *Journal of Sound and Vibration*, in press; doi:10.1016/j.jsv.2004.07.031.
[17] D.K. Cheng, *Field and Wave Electromagnetics*, Addison-Wesley, Reading, MA, 1992.
[18] D.J. Inman, *Engineering Vibration*, Prentice-Hall, Englewood-Cliffs, NJ, 1994.